



Article

A Typical Small Watershed in Southwestern China Is Demonstrated as a Significant Carbon Sink

Wenguang Chen ^{1,2}, Yafeng Lu ^{1,*}, He Yin ³, Xiaokang Zhou ^{1,2}, Zhengyang Li ^{1,2} and Yanguo Liu ⁴

- ¹ Institute of Mountain Hazards and Environment, Chinese Academy of Sciences, Chengdu 610041, China
- ² University of Chinese Academy of Sciences, Beijing 100049, China
- Department of Geography, Kent State University, 325 S. Lincoln Street, Kent, OH 44242, USA; hyin3@kent.edu
- Mianyang Science and Technology City Division, the National Remote Sensing Center of China, Southwest University of Science and Technology, Mianyang 621010, China; liuyg@swust.edu.cn
- * Correspondence: luyafeng@imde.ac.cn

Abstract: Small watersheds are fundamental units for natural processes and social management in Southwestern China. Accurately assessing carbon sinks in small watersheds is crucial for formulating carbon sink management policies. However, there has been a lack of assessment of the dynamics of carbon fluxes in the major ecosystems of small watersheds. Here, we selected the Reshuihe River watershed, which is a typical small watershed in Southwestern China, to measure carbon fluxes using eddy covariance systems for two years (October 2021 to September 2023) from three major ecosystems, namely forest, cropland, and non-timber forest. We compared variations and controlling factors of net ecosystem exchange (NEE), gross primary productivity (GPP), and ecosystem respiration (Re) among different ecosystems, and estimated annual watershed carbon flux based on the land cover areas of the three ecosystems. This study found that three ecosystems were net annual carbon sinks during the study period. Forest was the strongest (-592.8 and -488.1 gC m⁻² a⁻¹), followed by non-timber forest $(-371.0 \text{ gC m}^{-2} \text{ a}^{-1})$, and cropland was the smallest $(-92.5 \text{ and } -71.6 \text{ gC m}^{-2} \text{ a}^{-1})$, after taking fallow period into account. Weeds were a significant source of carbon flux in non-timber forest ecosystems. It was also found that variations in daily NEE were controlled by photosynthetically active radiation and soil volumetric water content, with weak effects related to temperature also being observed. However, when the temperature exceeded 21 °C, GPP and Re were significantly reduced in cropland. Finally, it was discovered that the total carbon sink of the three ecosystems in the watershed for one year was -52.15 Gg C. Overall, we found that small watersheds dominated by forest ecosystems in Southwestern China have a strong carbon sink capacity.

Keywords: small watershed; carbon fluxes; forest-cropland-non-timber forest ecosystems; eddy covariance; path analysis



Citation: Chen, W.; Lu, Y.; Yin, H.; Zhou, X.; Li, Z.; Liu, Y. A Typical Small Watershed in Southwestern China Is Demonstrated as a Significant Carbon Sink. *Land* **2024**, *13*, 458. https://doi.org/10.3390/ land13040458

Academic Editor: Nick B. Comerford

Received: 24 February 2024 Revised: 28 March 2024 Accepted: 2 April 2024 Published: 3 April 2024



Copyright: © 2024 by the authors. Licensee MDPI, Basel, Switzerland. This article is an open access article distributed under the terms and conditions of the Creative Commons Attribution (CC BY) license (https://creativecommons.org/licenses/by/4.0/).

1. Introduction

Southwestern China is rich in forests and agroecosystems and has strong carbon sink capacity in its terrestrial ecosystems [1,2]. Ecosystem carbon uptake is considered to be one of the most cost-effective methods for mitigating human carbon emissions [3]. Therefore, it is crucial to protect and enhance the carbon sink capacity of ecosystems in the Southwestern region to achieve the strategic goals of a carbon peak before 2030 and carbon neutrality before 2060. As independent natural catchment units [4], small watersheds act as a bridge between the site scale and the regional scale and are also important natural ecological and social functional areas. Southwestern China is made up of many small watersheds. To understand the functions of carbon sources and sinks in these watersheds and to formulate regional carbon sink management measures, it is essential to accurately estimate carbon fluxes from major ecosystems in small watersheds.

Currently, methods for carbon estimation include both 'top-down' and 'bottom-up' approaches [5]. The 'top-down' approach mainly refers to the atmospheric inversion

method. This method utilizes an atmospheric transport model and CO₂ concentration, in conjunction with carbon emissions from human activities, to estimate the regional carbon sink. However, carbon flux data based on the atmospheric inversion method has low spatial resolution and cannot accurately differentiate carbon fluxes among different ecosystems [6], thus making it difficult to apply this method to assess the carbon budget of small watersheds. 'Bottom-up' approaches mainly include the application of process-based ecosystem models and the eddy covariance method [5]. Ecosystem process models simulate the carbon cycle with drivers to estimate carbon flux data across multiple timescales; however, there are uncertainties in the model parameters [6], which makes it more difficult for the models to accurately obtain carbon flux data in small watersheds. Eddy covariance is a method of directly observing the net carbon exchange between ecosystems and the atmosphere through in-situ monitoring [7]. These observations are then scaled up to determine the regional carbon balance [8,9]. In recent years, studies have shown that 'top-down' estimates of carbon sinks in Southwestern China are highly uncertain, and that the size of the land sink in this region has been estimated differently [10,11]. Therefore, it is imperative to conduct more accurate carbon flux observations using eddy covariance in Southwestern China.

The characteristics of small watersheds determine the complexity of carbon flux studies. On the one hand, various ecosystems have their own unique structures and functions, and all simultaneously exchange carbon with the atmosphere as either carbon sources or sinks, leading to large uncertainties in the estimation of carbon flux components [4,12]. On the other hand, changes in carbon fluxes in different ecosystems may be correlated due to similar meteorological conditions within the watershed. Therefore, to accurately assess the carbon sinks of small watersheds containing multiple ecosystems, it is necessary to monitor ecosystem–atmosphere carbon fluxes for major ecosystems in the region [13]. Furthermore, researchers are currently not only concerned with the carbon source/sink function of ecosystems, but also with the responses of carbon flux to ecological environmental factors [14–16]. Despite similar meteorological factors within the same watershed, different ecosystems may respond differently to extreme climate events [17,18]. Therefore, understanding the relationships between carbon fluxes and environmental factors in different ecosystems will help to develop and validate biophysical models.

The study area selected for this research is the Reshuihe River watershed in Southwestern China. The watershed is mainly composed of forest, cropland, and non-timber forest ecosystems, which account for over 75% of the total area. Carbon flux data from the three ecosystems were continuously monitored for two years (October 2021 to September 2023) using eddy covariance systems, and environmental factor data were recorded at each site using meteorological instruments. The annual carbon balance was estimated based on observational data combined with the area of different ecosystems in the small watershed. The specific objectives of this study are as follows: (1) characterize carbon fluxes (including the net ecosystem exchange (NEE), gross primary productivity (GPP), and ecosystem respiration (Re)) in forest, cropland, and non-timber forest ecosystems; (2) determine the drivers of NEE, GPP, and Re in different ecosystems and the effects of high temperature on carbon fluxes; and (3) combine the NEE data of the three ecosystems to determine the carbon source/sink function of the watershed.

2. Materials and Methods

2.1. Site Area and Flux Sites

The study area is located in the Reshuihe River watershed in Liangshan Yi Autonomous Prefecture, Sichuan Province, Southwestern China (Figure 1), with a total area of 151 km². The study area is characterized by a subtropical alpine climate, with an average annual temperature of about 13.1 °C and a long-term average annual precipitation of about 1075 mm. The wet season starts in May or June and ends in September each year, during which more than 80% of the total annual precipitation falls. The ecosystems in the watershed primarily consist of forest, cropland, and non-timber forest, accounting for

75.4% of the total watershed area. The dominant tree species in the forest ecosystem is *Pinus yunnanensi*, the cropland is mainly planted with potatoes and maize, and the regional non-timber forest focuses on the cultivation of *Zanthoxylum bungeanum Maxim*.

Three eddy covariance systems were deployed at locations in the watershed where forest, cropland, and non-timber forest were evenly distributed. Figure 1 and Table 1 show the basic information of the three eddy covariance sites, such as the location, altitude, vegetation types, etc.

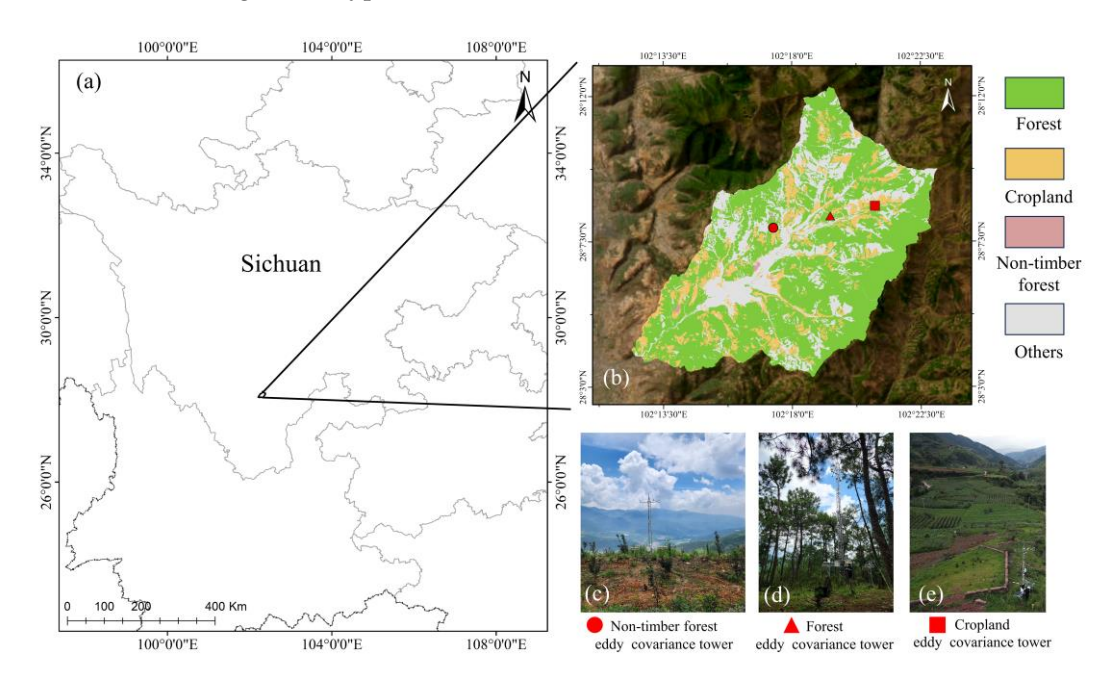


Figure 1. (a) Location of the Reshuihe River watershed in Southwestern China; (b) watershed boundary and the distribution of forest, cropland, and non-timber forest within the watershed; eddy covariance systems installed in (c) non-timber forest, (d) forest, and (e) cropland.

Table 1. Overview of eddy covariance sites for forest, cropland, and non-timber forest in the Reshuihe
River watershed.

Sites	Geographical Location	Altitude (m)	Vegetation Types	Observation Height (m)	Observation Time
Forest	28°8′18.4″ N, 102°19′20.2″ E	2343	Pinus yunnanensis dominates	12	October 2021–September 2023
Cropland	28°8′36.0″ N, 102°20′53.9″ E	2359	Potatoes and maize	6	October 2021–September 2023
Non-timber forest	28°7′55.6″ N, 102°17′20.6″ E	2218	Zanthoxylum bungeanum Maxim	6	October 2021–September 2023

2.2. Eddy Covariance and Ancillary Data

Three sets of integrated CO₂/H₂O open-path gas analyzers and three-dimensional sonic anemometers (IRGASON, Campbell Scientific Inc., Logan, UT, USA) were used to observe carbon flux between forest, cropland, and non-timber forest ecosystems and the atmosphere, as well as the three wind speed components (uy, uz, and ux). The instruments were installed on flux towers at three sites, with the instrument installation height at the forest site being 12 m (Figure 1d), and the instrument installation height at the cropland site (Figure 1e) and non-timber forest site (Figure 1c) being 6 m. Air temperature and relative humidity sensors (HMP155, Vaisala, Helsinki, Finland), photosynthetically active radiation sensors (LI190R, Campbell Scientific Inc., Logan, UT, USA), and tipping-bucket rain gauges (TE525MM; Campbell Scientific Inc., Logan, UT, USA), which record precipitation, were

Land **2024**, 13, 458 4 of 21

also installed on the flux towers at each site to record meteorological data. Soil temperature and moisture were obtained using time-domain reflectometer (TDR) moisture sensors (True TDR-315, Acclima, Inc., Meridian, ID, USA) installed in the soil at a depth of 10 cm near each flux tower. VPD was computed based on the air temperature and relative humidity measurements. A data collector (CR1000X, Campbell Scientific Inc., Logan, UT, USA) collected the carbon fluxes and 3D wind speed data at 10 Hz, as well as the averages or sums of meteorological data recorded at 30 min intervals. The instrument was maintained and inspected at an average of every 45 days.

In this study, we collected carbon flux and environmental factor data from October 2021 to September 2023 at forest, cropland, and non-timber forest sites. Due to field instrument failures and power supply problems, some data were missing, including soil temperature data at forest site from 9 January 2022 to 25 June 2022, and carbon flux data and some meteorological data at the non-timber forest site from 1 March 2022 to 13 May 2022.

2.3. Eddy Covariance Data Processing, Gap Filling and Flux Partitioning

Eddypro 7.0.9 software (LI-COR Biosciences, Lincoln, NE, USA) was used to process the raw 10 Hz flux data. Data processing flow was as follows: data quality control was carried out according to the method recommended by Vickers et al. [19], and a double rotation [20] (forest and cropland sites) and planar fit coordinate rotation [21] (non-timber forest site) were used to eliminate the influence of instrument tilt or terrain irregularity on airflow. The effects of air density fluctuations due to heat and water vapor transfer were corrected using Webb-Pearman-Leuning (WPL) correction [22]. Further, flux data were deleted for precipitation time periods. A quality check was performed on the flux data based on internal turbulence tests [23], removing low quality flux data marked as 2. To mitigate the impact of low turbulence on flux data at night time (shortwave incoming global radiation less than 10 W m $^{-2}$), the friction velocity (u*) thresholds (0.26–0.37 m s $^{-1}$ for forest dataset, $0.19-0.21 \text{ m s}^{-1}$ for cropland dataset, and $0.23-0.25 \text{ m s}^{-1}$ for non-timber forest dataset) determined based on the moving point test (MPT) were applied to filter nighttime carbon flux data [24]. After conducting quality control and u* filtering, the carbon flux datasets for the three sites over two years showed a percentage of missing data ranging from 33.9% to 39.6% (Table 2). The percentage of missing eddy covariance data typically ranged from 20% to 60% and was mainly concentrated at night [25]. Therefore, the rates of missing data at our three sites are reasonable.

Table 2. Percentage of carbon flux data gaps for three eddy covariance sites after quality control and u^* filtering.

Sites	October 2021 to September 2022 (%)	October 2022 to September 2023 (%)	Averaged-Gaps (%)
Forest	41.8	25.9	33.9
Cropland	37.2	32.7	35.0
Non-timber forest	46.8	42.4	39.6

Notes: The count does not include data from non-timber forest site between 1 March and 13 May 2022.

Missing data was filled using marginal distribution sampling (MDS) [26]. The MDS method has been widely used to fill carbon flux data gaps [18,25,27]. It takes into account the temporal autocorrelation of fluxes and the covariance between meteorological variables and fluxes, and uses shortwave incoming global radiation (Rg), air temperature (T_{air}), and vapor pressure deficit (VPD) to fill the half-hourly NEE. A more detailed description can be found in the paper by Wutzler et al. [27]. The gap filling process was performed using the REddyProC package [27].

Land **2024**, 13, 458 5 of 21

Half-hourly NEE was partitioned into GPP and Re. At night, NEE is equal to Re, when GPP is equal to 0. Based on the half-hourly nighttime data, the relationship between Re and T_{air} was established using Equation (1) [28]:

$$Re = R_{ref} \cdot exp \left(E_0 \cdot \left(\frac{1}{T_{ref} - T_0} - \frac{1}{T_{air} - T_0} \right) \right) \tag{1}$$

where Re (μ mol m⁻² s⁻¹) is the ecosystem respiration, R_{ref} (μ mol m⁻² s⁻¹) is the ecosystem respiration rate at a reference temperature (T_{ref}) of 15 °C, T₀ is kept constant at -46.02 °C, E₀ (K) is the activation energy, and T_{air} is air temperature. After Re and T_{air} for the nighttime data were linked through Equation (1), the Re values could be estimated as a function of T_{air} during the daytime. Subsequently, GPP could be calculated using Equation (2):

$$GPP = Re - NEE$$
 (2)

Both Re and GPP were calculated using the REddyProC package [27]. This paper follows the convention that, when NEE is negative, the ecosystem is acting as a net carbon sink; when NEE is positive, it is a net carbon source.

2.4. Response Curves for Photosynthesis

To assess the influence of PAR and SVWC on carbon exchange, we divided SVWC of the three ecosystems into three change intervals based on the average value of SVWC during the dry seasons (October 2021–April 2022 and October 2022–May 2023) and wet seasons (May 2022–September 2022 and June 2023–September 2023), and the relationships between half-hourly NEE and PAR during daytime hours at different intervals were analyzed separately. The Michaelis–Menten model [29,30] (Equation (3)) was used to fit the daytime NEE and PAR to the light response curves:

$$NEE = -\frac{\varepsilon \times A_{max} \times PAR}{\varepsilon \times PAR + A_{max}} + Re$$
 (3)

where ε (µmol CO₂/µmol PAR) is the apparent quantum yield, A_{max} (µmol CO₂ m⁻² s⁻¹) is apparent maximum photosynthetic rate, and Re (µmol CO₂ m⁻² s⁻¹) is the ecosystem respiration. To avoid data scattering, the analysis used half-hour NEE averages in increments of 60 µmol m⁻² s⁻¹ PAR.

2.5. Path Analysis

Carbon flux is controlled by various environmental factors. However, environmental factors are essentially interrelated, and it is difficult for common correlation analysis methods to truly identify the main factors that control ecosystem carbon absorption and release [31]. Therefore, our study used path analysis to investigate the relationships between carbon fluxes (NEE, GPP, and Re) and major environmental factors in forest, cropland, and non-timber forest ecosystems at the daily scale.

Path analysis, a statistical method for assessing the relationships between different variables based on priori causal knowledge, has been widely used in studies analyzing carbon fluxes and environmental factors [18,32]. Our study selected photosynthetically active radiation, air temperature, and soil volumetric water content as explanatory variables for NEE and GPP, and selected air temperature and soil volumetric water content as the explanatory variables for Re. All variables were standardized using Z-score, and the R package 'lavaan' [33] was used to conduct path analysis. A total of nine path analysis models were constructed.

Land **2024**, 13, 458 6 of 21

3. Results

3.1. Environmental Conditions

Environmental factors in the forest, cropland, and non-timber forest sites exhibited obvious seasonal variations (Figure 2). The results showed that (1) PAR was low at the beginning of the year and trended upwards thereafter, peaking in June and July and then gradually declining; (2) the trends of $T_{\rm air}$ and $T_{\rm soil}$ exhibited a unimodal pattern in one year; however, the fluctuation of $T_{\rm soil}$ was smaller. The daily minimum of $T_{\rm air}$ occurs from January to February, and the maximum occurs from May to July; and (3) SVWC was found to be closely related to precipitation. In both years, the wet seasons were from May to September and from June to September, respectively, and the proportion of wet season precipitation to total annual precipitation was more than 80%. Additionally, VPD was also affected by variability in precipitation.

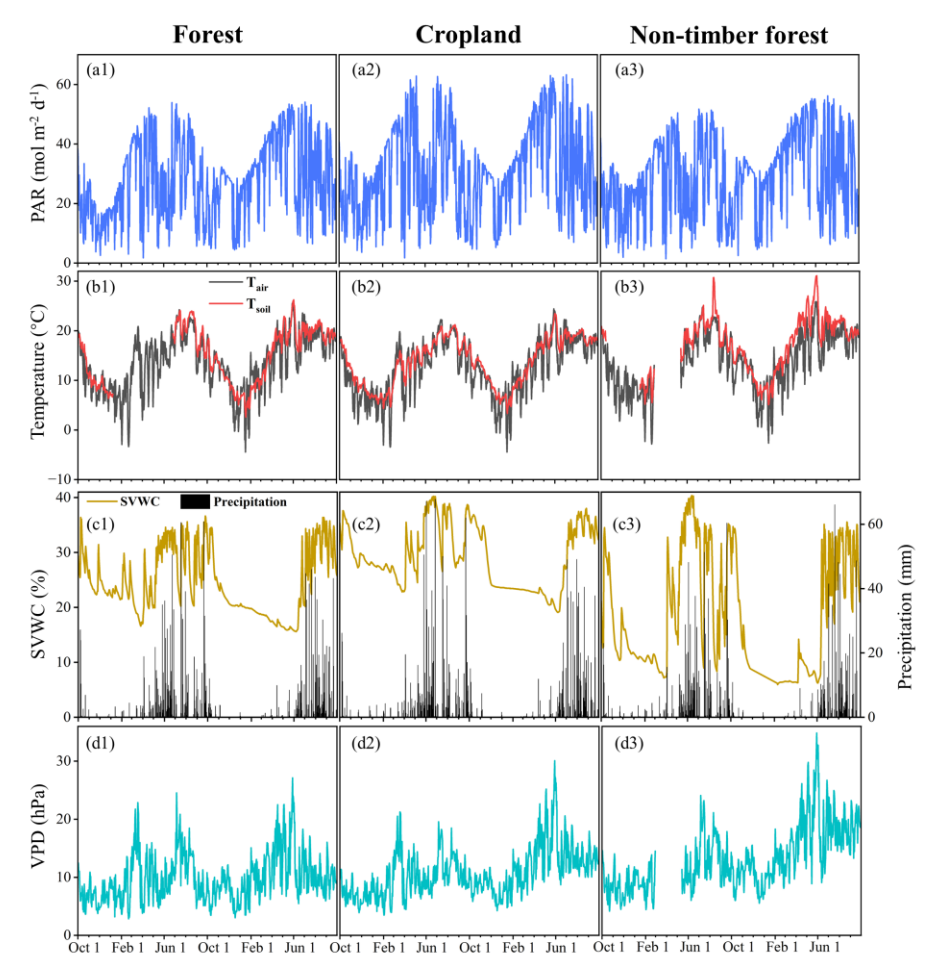


Figure 2. Seasonal variations of meteorological elements in forest, cropland, and non-timber forest sites in the Reshuihe River watershed between October 2021 and September 2023, including (a1–a3) daily summed photosynthetically active radiation (PAR); (b1–b3) daily mean air temperature (T_{air}) and soil temperature (T_{soil}) at -10 cm; (c1–c3) soil volumetric water content (SVWC) at -10 cm and daily summed precipitation; and (d1–d3) daily mean vapor pressure deficit (VPD).

Overall, the watershed was characterized by precipitation and heat during the same period. Environmental factors were higher between May and September each year and relatively lower during the rest of the year. Furthermore, the forest and cropland sites exhibited fewer differences in environmental factors due to their similar elevation (about 2400 m). The non-timber forest site was situated at a relatively lower elevation (2218 m) and had higher mean annual temperatures, less annual precipitation, and lower mean annual SVWC.

Land **2024**, 13, 458 7 of 21

3.2. Variations in Carbon Fluxes

3.2.1. Diurnal Variations

Seasonal and annual mean diurnal variation characteristics of carbon fluxes at each site are shown in Figure 3. Net carbon uptake was higher from July to September, with longer durations of negative daytime NEE values. The daytime NEE values for the forest site were generally smaller than those of the other two sites, indicating that its carbon sink capacity was stronger.

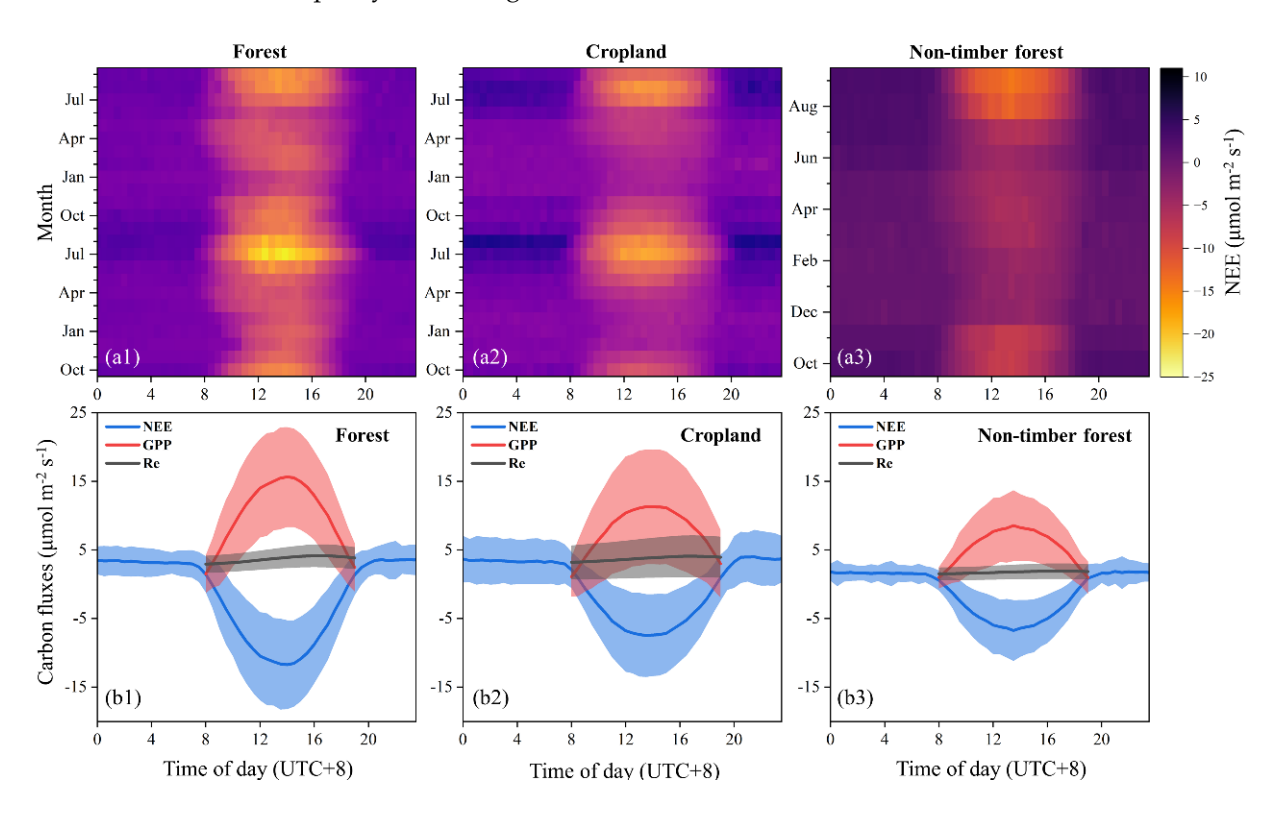


Figure 3. Diurnal variation characteristics of carbon fluxes in forest and cropland sites from October 2021 to September 2023 and in non-timber forest site from October 2022 to September 2023, including (a1–a3) diurnal variation of NEE in different months, and (b1–b3) diurnal variation of NEE, GPP, and Re during the corresponding data periods. The shaded areas represent the standard deviations for each half-hourly value.

Diurnal variations of NEE and GPP were consistent, and both exhibited typical single-peak curves during the daytime. Over a 24 h cycle, the minimum values of NEE and the maximum values of GPP appeared at 13:30–14:00. The net carbon release stage occurred at night. The peak occurrence of daytime Re was delayed by 2.5–3 h compared to the GPP.

3.2.2. Seasonal and Annual Carbon Fluxes

Carbon fluxes (NEE, GPP, and Re) at the three sites over the course of two years are shown in Figure 4. The annual NEE values were -592.8 and -488.1 gC m⁻² a⁻¹ for forest, and -92.5 and -71.6 gC m⁻² a⁻¹ for cropland, respectively. The carbon sink for non-timber forests was -371.0 gC m⁻² a⁻¹ from October 2022 to September 2023.

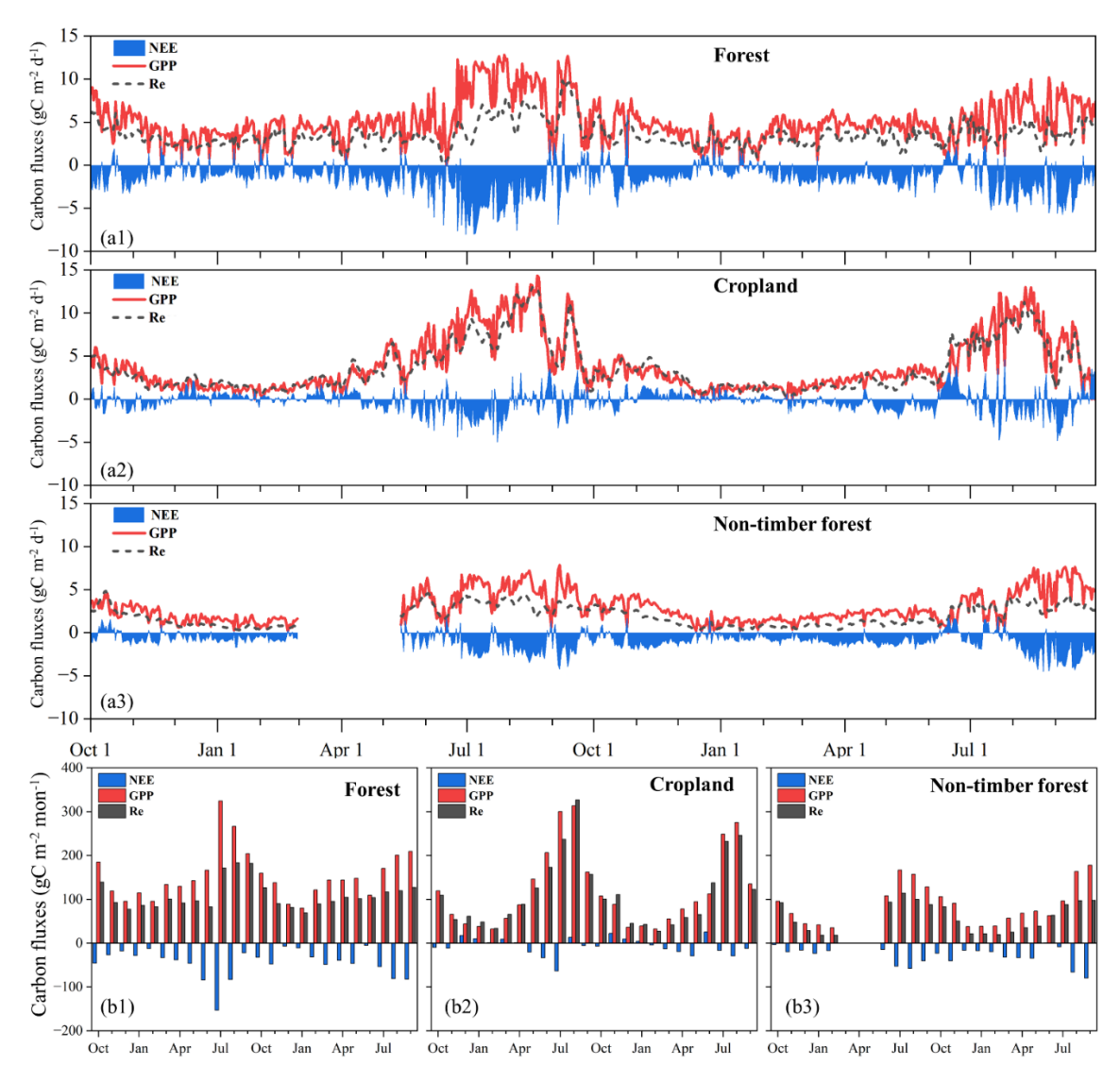


Figure 4. Changes in (a1–a3) daily and (b1–b3) monthly NEE, GPP, and Re in forest, cropland, and non-timber forest sites from October 2021 to September 2023.

The variation in daily NEE at the forest site over the two-year period ranged from -8.0 to 5.9 gC m⁻² d⁻¹. Monthly NEE values were negative for 24 months, with the lowest value occurring in July 2022. GPP and Re values increased rapidly from around May each year, peaked in July and August, and then gradually decreased. Daily NEE at the cropland site varied within the range of -5 to 4.6 gC m⁻² d⁻¹. In the two-year period, the site acted as a carbon sink for 197 and 213 days, respectively. Potatoes and maize were planted around the observation site in mid-March and mid-May, which facilitated carbon uptake. There were two phases of decline in GPP and Re after the maturation of potatoes in late August and maize in mid-September. From October 2022 to September 2023, the minimum and maximum daily NEE values at the non-timber forest site were -4.5 and 1.9 gC m⁻² d⁻¹, respectively. Carbon sinks were observed on 88% of the days during this period. Monthly NEE was only slightly positive (0.8 gC m⁻² mon⁻¹) in June 2023, and negative in the remaining months. Mid-July was the ripening and harvesting period of Zanthoxylum bungeanum Maxim fruits. At this time, NEE increased (i.e., carbon uptake decreased) and GPP and Re decreased. Subsequently, there was another period of decline in NEE. The defoliation of Zanthoxylum bungeanum Maxim trees started in early November, and both GPP and Re remained low afterwards.

Furthermore, significant positive correlations were found between daily changes in NEE across the various ecosystems (p < 0.001, Figure 5). The correlation between NEE in each of the two ecosystems was consistently greater than 0.45 when analyzing data from the two years of the study period.

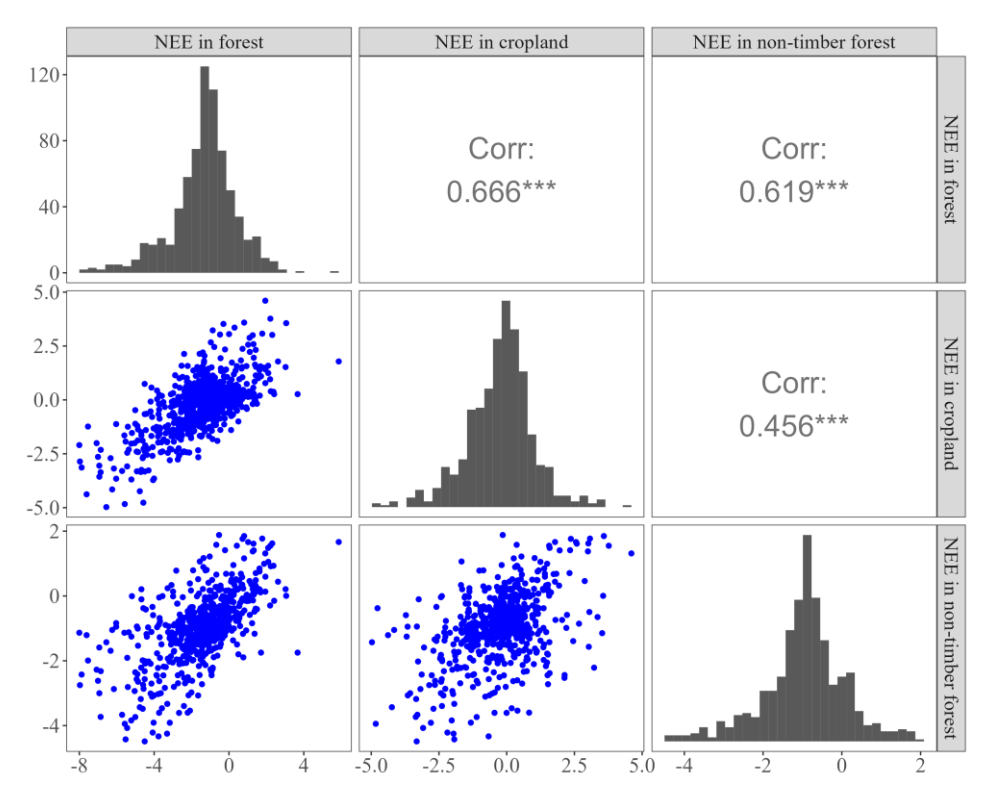


Figure 5. Correlation matrix between daily NEE in forest, cropland, and non-timber forest sites from October 2021 to September 2023. *** p < 0.001.

3.3. Carbon Fluxes in Relation to Environmental Factors

3.3.1. Drivers of Carbon Fluxes in Different Ecosystems

Daily carbon fluxes in different ecosystems were controlled by different combinations of environmental factors (Figure 6). The results of path analysis showed that PAR was the most important factor controlling NEE, with the magnitudes of the total effects of forest, cropland, and non-timber forest being -0.7, -0.59, and -0.55, respectively. We also observed significant negative correlations (p < 0.001) between SVWC and NEE. This suggested that higher PAR and SVWC could favor net carbon uptake. Interestingly, the effects of $T_{\rm air}$ on NEE were weak, and the relationship between NEE and $T_{\rm air}$ in non-timber forest did not pass the significance test (p > 0.05).

PAR, SVWC, and T_{air} were all significantly positively correlated with GPP (p < 0.001), but there were differences in path coefficients. Path coefficients between PAR and GPP were the largest at the forest site. However, at the cropland and non-timber forest sites, SVWC was the best explanatory variable for changes in daily GPP. In contrast to NEE, the daily variation of T_{air} had significant effects on GPP.

Daily variations in Re were influenced by T_{air} and SVWC. SVWC had a greater effect on Re than T_{air} at the non-timber forest site (0.71), while T_{air} was more important at the forest and cropland sites (0.61 and 0.55).

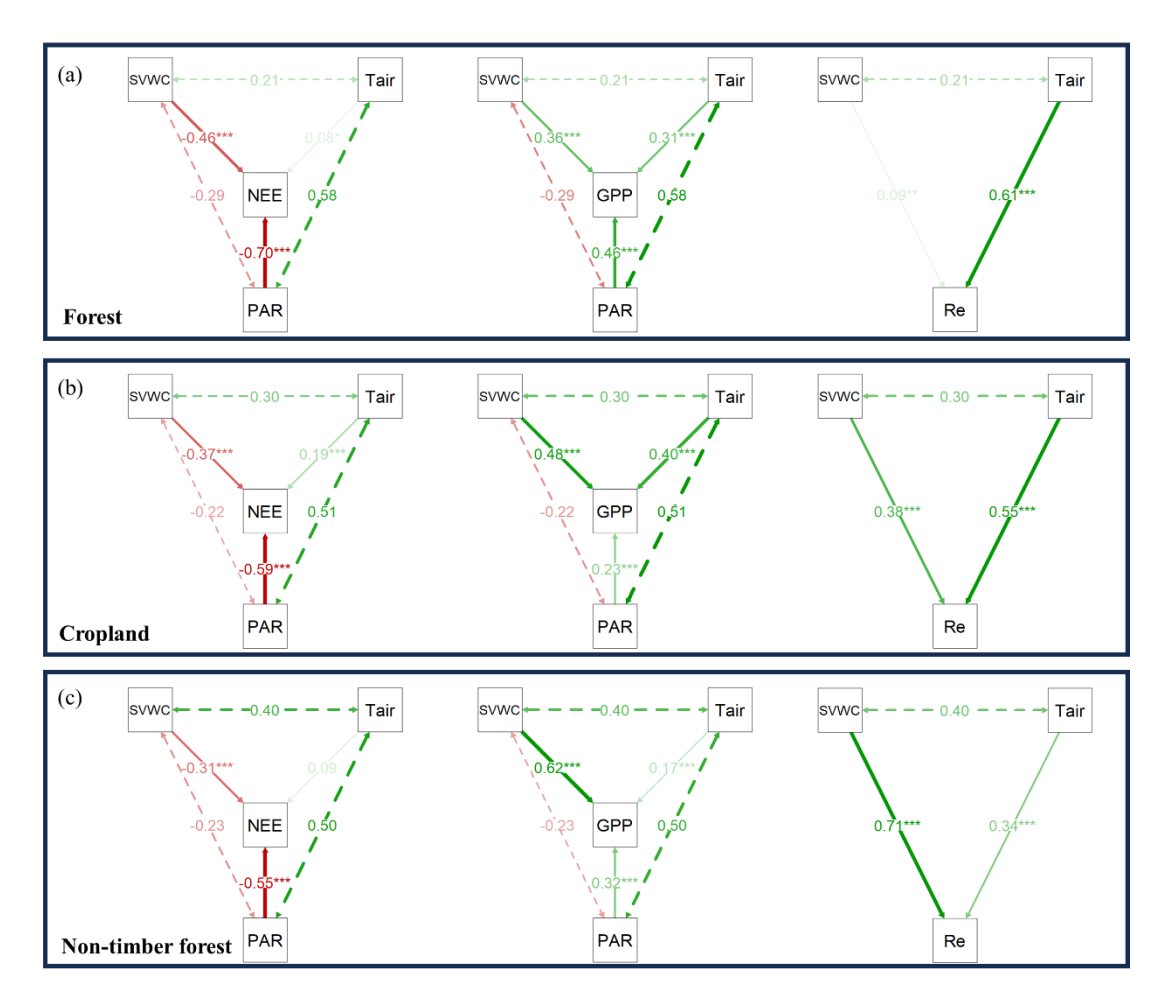


Figure 6. Path diagrams illustrating the effects of PAR, SVWC, and T_{air} on NEE (left panels), GPP (middle panels), and Re (right panels) in (a) forest, (b) cropland, and (c) non-timber forest sites. The values on the arrows indicate the path coefficients. The width of the arrows is proportional to the strength of the path coefficients, and the green and red colors indicate positive and negative effects, respectively. Data were available from October 2021 to September 2023 for forest and cropland sites, and from October 2022 to September 2023 for the non-timber forest site. * p < 0.05; *** p < 0.01; *** p < 0.001.

3.3.2. Responses of Carbon Fluxes to PAR, SVWC and Tair

In this study, the Michaelis–Menten equation (Equation (3)) was used to fit the relationships between NEE and PAR during the daytime (shortwave incoming global radiation > $10~W~m^{-2}$) under different SVWC conditions for different sites (Figure 7). The results showed that all daytime NEE decreased with increases in PAR, and the rate of change of daytime NEE decreased with increases in PAR. Furthermore, the effects of PAR on daytime NEE were also regulated by SVWC. The light response curves of different sites differed under different SVWC conditions. In general, the values of A_{max} , ε , and Re of the light response curves were higher under high SVWC conditions (>29%, 33%, and 26%, respectively) (Table 3).

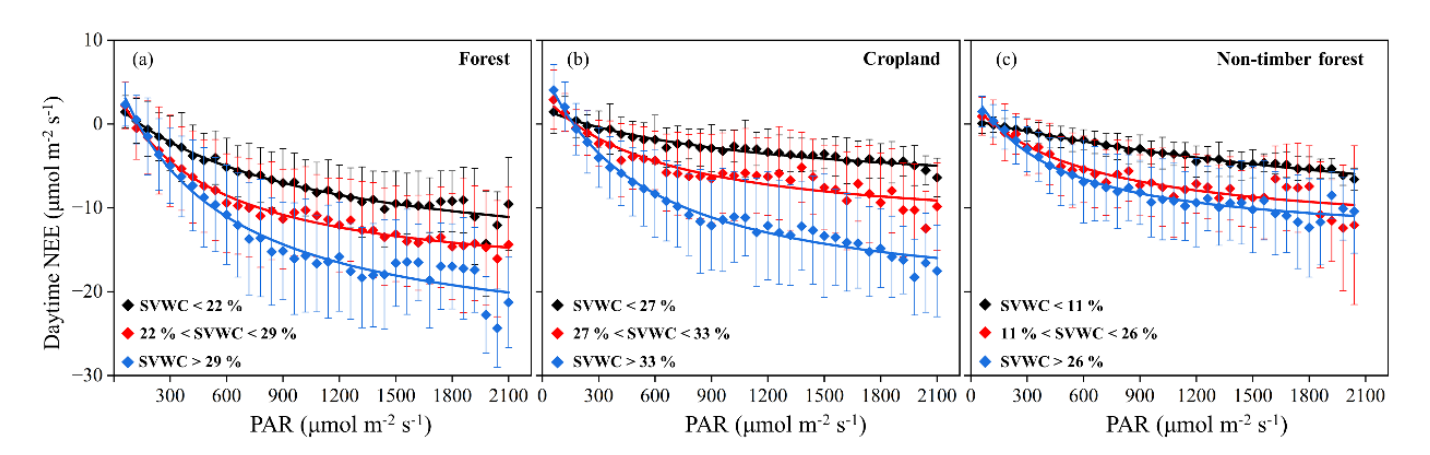


Figure 7. Relationships between daytime NEE and PAR under different SVWC conditions for the (a) forest, (b) cropland, and (c) non-timber forest sites. Daytime half-hourly NEE data were averaged at PAR intervals of $60 \, \mu \text{mol m}^{-2} \, \text{s}^{-1}$. Fitted curves were rectangular hyperbolic based on Equation (3), and the fitted parameters are shown in Table 2; error bars indicate standard errors. Data were available from October 2021 to September 2023 for forest and cropland sites and from October 2022 to September 2023 for the non-timber forest site.

Table 3. Fitting parameters, standard errors, and coefficients of determination (R^2) of Equation (3) for forest, cropland, and non-timber forest sites under different SVWC conditions in Figure 7. Significant differences in a given parameter among the three levels of SVWC are indicated by different letters (p < 0.05, one-way ANOVA and Tukey's HSD test).

Sites		ε (μmol CO ₂ μmol ⁻¹ PAR)	A_{max} (μ mol CO ₂ m^{-2} s ⁻¹)	Re $(\mu mol\ CO_2 \ m^{-2}\ s^{-1})$	R ²
Forest	SVWC < 22% 22% < SVWC < 29% SVWC > 29%	0.0200 ± 0.0002 a 0.0485 ± 0.0125 a 0.0608 ± 0.0307 a	19.96 ± 3.02 a 23.80 ± 3.04 a 33.41 ± 1.99 b	2.43 ± 1.94 a 4.56 ± 2.09 a 6.38 ± 0.21 a	0.94 0.98 0.95
Cropland	SVWC < 27% 27% < SVWC < 33% SVWC > 33%	0.0091 ± 0.0011 a 0.0258 ± 0.0067 ab 0.0527 ± 0.0148 b	10.38 ± 0.39 a 16.48 ± 3.83 a 28.49 ± 3.48 b	1.77 ± 1.43 a 3.51 ± 1.45 ab 6.66 ± 1.02 b	0.95 0.88 0.97
Non-timber forest	SVWC < 11% 11% < SVWC < 26% SVWC > 26%	0.0050 ± 0.0017 a 0.0256 ± 0.0039 ab 0.0455 ± 0.0163 b	17.42 ± 2.12 a 15.96 ± 4.18 a 18.50 ± 3.59 a	0.49 ± 0.38 a 2.57 ± 1.98 ab 4.47 ± 0.32 b	0.98 0.85 0.96

Figure 8 illustrated the relationships between carbon fluxes with daily mean T_{air} at different sites. GPP and Re tended to zero when T_{air} was below 0 °C. When T_{air} < 21 °C in cropland site, GPP and Re increased with increasing T_{air} ; however, when T_{air} > 21 °C, GPP and Re decreased significantly (p < 0.01) compared to 18 °C < T_{air} < 21 °C. Overall, GPP and Re increased with T_{air} in forest and non-timber forest sites, and no significant changes were observed in GPP and Re when T > 21 °C.

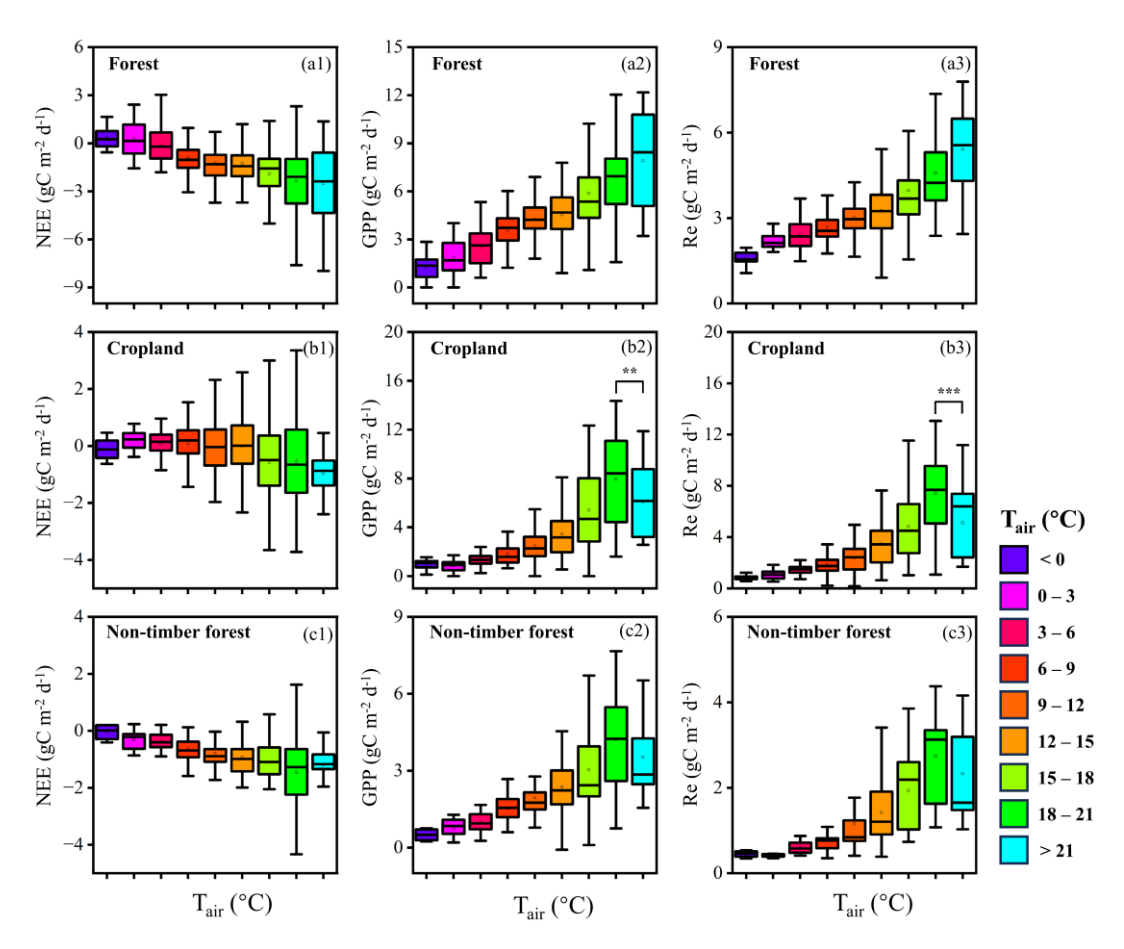


Figure 8. Relationships between NEE, GPP, and Re with T_{air} for the (a1–a3) forest, (b1–b3) cropland, and (c1–c3) non-timber forest sites. Boxplots represent the 50% distribution percentile, horizontal lines in the boxes indicate the median, and vertical bars indicate a 99% distribution. Each color represents an interval in the distribution of T_{air} . Data were available from October 2021 to September 2023 for forest and cropland sites, and from October 2022 to September 2023 for the non-timber forest site. ** p < 0.01; *** p < 0.001.

3.4. Total Annual Carbon Fluxes in the Three Ecosystems in the Reshuihe River Watershed

To estimate the regional carbon budget for this small watershed in our study area, the annual carbon fluxes observed in forest, cropland, and non-timber forest sites were multiplied by the area of the corresponding land use type to obtain the annual carbon budget of each ecosystem within the small watershed. The results showed that the annual carbon uptake in the watershed was -50.3, -1.7, and -0.15 Gg C for forest, cropland, and non-timber forest ecosystems, respectively. These three ecosystems accounted for 75.4% of the total area of the watershed, with a total carbon sink of -52.15 Gg C in one year (Figure 9).

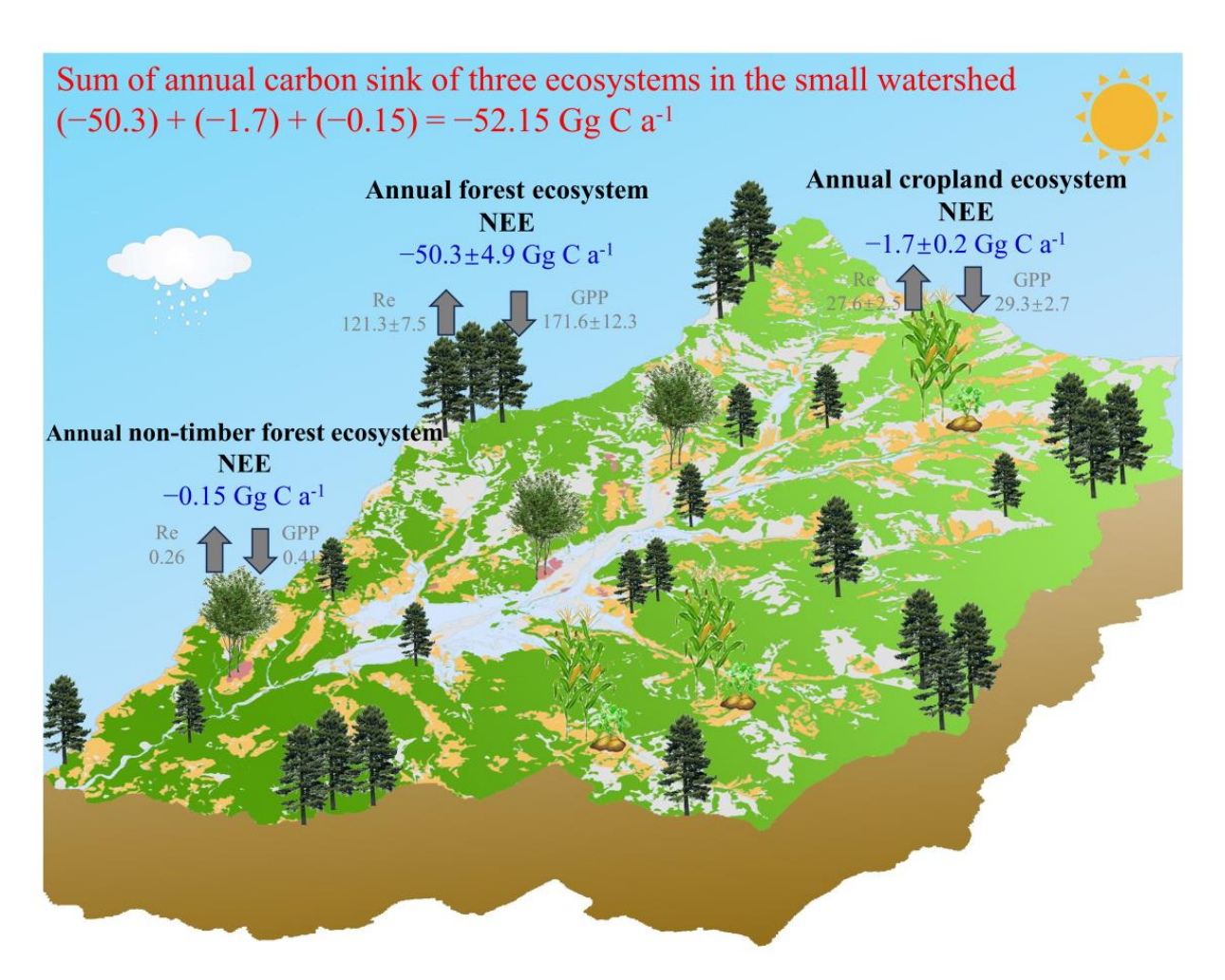


Figure 9. Conceptual diagram of the estimated annual carbon budget of forest, cropland, and non-timber forest ecosystems, and the sum of the total inter-annual carbon sink of the three ecosystems in the Reshuihe River watershed. Numbers after the \pm symbols represent the standard errors.

4. Discussion

4.1. Effects of Environmental Factors on Carbon Fluxes

Ecosystem carbon fluxes are affected to varying degrees by various environmental factors (e.g., radiation, temperature, and moisture) [17,34,35]. In the Reshuihe River watershed, PAR is the most important environmental factor influencing the carbon-sink capacity of forest, cropland, and non-timber forest ecosystems. Among them, the strong correlation between NEE and radiation in forest ecosystems has been widely recognized in previous studies [16,18,36]. Similar results show that PAR is the dominant factor controlling the variation in daily NEE in cropland ecosystems. This was verified in a wheat–maize rotation system in the Huaibei Plain of China [37], and a maize field in the arid areas upstream of the Yellow River Basin [38]. In addition, the carbon-sink capacity of the non-timber forest ecosystem (*Zanthoxylum bungeanum Maxim* plantation) in this study area was closely related to PAR, which is consistent with the light preference of *Zanthoxylum bungeanum Maxim* growth [39].

Soil volumetric water content regulates photosynthesis and respiration processes by affecting plant transpiration and soil respiration [40,41], thus determining carbon cycle. In different ecosystems of our study area, SVWC is significantly positively correlated with GPP. The reason for this is that more SVWC enhances the photosynthetic capacity of plants (Figure 7 and Table 2). Since soil drought inhibits the activities of plant roots and soil microorganisms, leading to decreased soil respiration [42], more SVWC is beneficial for reducing drought stress. Moreover, increases in SVWC correspond to smaller NEE values,

i.e., stronger carbon sinks, suggesting that SVWC promotes GPP more than Re, resulting in greater carbon absorption than carbon release.

The effects of air temperature on daily NEE were small (Figure 6); however, its effects on GPP and Re were larger (Figures 6 and 8). In the coniferous forest ecosystems of our study area, the effect of Tair on the variation of daily NEE was weak (path coefficient was 0.08). However, Fei et al. found through long-term observations in the Yunnan Province, Southwestern China that temperature had a large effect on the monthly NEP in a subalpine coniferous forest ecosystem [17]. This discrepancy may be due to the different timescales used in the analyses. Here, it was found that carbon fluxes in cropland ecosystems in this study area were more susceptible to high temperatures. On the one hand, higher temperatures ($T_{air} > 21^{\circ}$) inhibit GPP in the cropland ecosystem. This phenomenon may be the result of plants adapting to greater evaporative demands and less soil moisture, where stomatal conductance is reduced at high temperatures, thus reducing GPP [43]. In addition, Tair is positively correlated with VPD, leading to a high VPD at high temperatures, and a high VPD causes GPP to decrease [44,45]. On the other hand, Re increases with T_{air} in the appropriate temperature range, but high temperatures $(T_{air} > 21^{\circ})$ suppress Re in the cropland ecosystem. Analyzing the effects of high temperatures on respiration is further complicated by the fact that ecosystem respiration comprises the respiration of plant roots, stems, and foliage, as well as the heterotrophic respiration of soil microorganisms [46]. Moreover, in the three ecosystems, GPP and Re are suppressed when temperatures are below 0 °C because low temperatures lead to processes such as reduced water and nutrient uptake, as well as stomatal closure [47], resulting in limited plant production [32,48].

Since the effects of temperature on NEE are relatively small compared to SVWC, we expect that the carbon sink capacity of forest, cropland, and non-timber forest ecosystems in the region will decrease in the future against the backdrop of rising temperatures and decreasing precipitation in Southwestern China [49]. It is important to note that this is only a preliminary extrapolation, as changes in carbon sinks are also subject to a combination of seasonality and other factors [17].

4.2. Carbon Flux Variability

In the Reshuihe River watershed, forest, cropland, and non-timber forest ecosystems serve as significant carbon sinks. The annual carbon sequestration capacity (per unit area) is in the following order: forest (-592.8, -488.1 gC m $^{-2}$ a $^{-1}$) > non-timber forest (-371.0 gC m $^{-2}$ a $^{-1}$) > cropland (-92.5, -71.6 gC m $^{-2}$ a $^{-1}$). In terms of seasonal variations, the factors that control NEE (including PAR, T_{air} , and SVWC) are more abundant during the wet seasons, resulting in a significant carbon sink during this period [15,17].

Forest ecosystems make up over 60% of the study area, which is dominated by coniferous forests. Compared to coniferous forests in other areas and different types of forests (such as coastal plain, dry tropical, temperate, and boreal, etc.) (Table 4), the forest in this study area was found to have a strong carbon sink capacity. This corroborates previous research that has shown that Southwestern China's forests are considered to have a strong carbon sink capacity [1,2]. Additionally, we observed a carbon sink in the forest site every month for two years. This phenomenon has been found in numerous forest ecosystems with strong carbon sinks, such as broadleaved forest ecosystems and subalpine coniferous forest ecosystems in the Yunnan Province, China [17], and evergreen forest ecosystems in South China [50].

Table 4. Comparison of carbon fluxes in different forest ecosystems.

Country	Area	Functional Type	Mean Annual NEE (gC m ⁻²)	Mean Annual GPP (gC m ⁻²)	Mean Annual Re (gC m ⁻²)	Reference
China	Liangshan	Subtropical, coniferous forest	-540	1845	1304	This study
China	Changbai Mountain	Temperate, coniferous forest	-169~-187	-	-	[51]
China	Lijiang	Cold-temperate, coniferous forest	-405	1392	987	[17]
Finland	Hyytiälä	Boreal, coniferous forest	-206	1,031	826	[52]
Israel	Yatir	Semi-arid, coniferous forest	-211	830	620	[53]
US	Arizona	Temperate, coniferous forest	-112	935	844	[54]
US	Washington	Temperate, coniferous forest	-32	1382	1350	[55]
US	North Carolina	Coastal plain, coniferous forest	-640	2719	2082	[56]
US	Florida	Subtropical, coniferous forest	-669	2490	1821	[57]
Netherlands	centre	Temperate, coniferous forest	-338	1221	1559	[58]
Brazil	semiarid lands	Dry tropical, deciduous and semi-deciduous forest	-169	415	246	[16]
Brazil	Jaru Biological Reserve	Tropical, broadleaved forest	-450	3413	2963	[59]
Canada	Saskatchewan	Boreal, broadleaved forest	-168	1252	1084	[60]

During the crop growth stage, cropland ecosystems exhibit a rapid increase in GPP and Re [61]. By comparing the annual NEE of cropland ecosystems in different locations (Table 5), we found that the carbon sink capacity of cropland in the Reshuihe River watershed was relatively weak. This is mainly due to the long fallow period of local cropland (about 6 months per year), during which carbon release from soil respiration reduces the annual carbon sink.

Table 5. Comparison of carbon fluxes in different cropland ecosystems.

Country	Area	Functional Type	Mean Annual NEE (gC m ⁻²)	Mean Annual GPP (gC m ⁻²)	Mean Annual Re (gC m ⁻²)	Reference
China	Liangshan	Potatoes and maize	-82	1437	1354	This study
China	Heihe river basin	maize	-536	-	-	[62]
China	North Plain	wheat and maize	-258	-	-	[63]
Canada	Breton	secale	-89	1242	1153	[25]
US	Ponca	wheat	-155	1395	1240	[64]
US	Nebraska	maize and soybean	-225	1201	976	[65]
Germany	Thuringia	wheat	-185~-245	-	-	[66]

Non-timber forest ecosystems have a strong carbon sink capacity. Moreover, the period of net carbon uptake after harvesting of *Zanthoxylum bungeanum Maxim* fruits was due to two main reasons: (1) The growth of *Zanthoxylum bungeanum Maxim* trees increased carbon fixation due to sufficient light and moisture, and (2) due to the lack of garden management

after harvesting, weeds (mainly ragweed) grew rapidly. Weed growth has been widely discussed as an important source of carbon fluxes in agroecosystems. For example, two years of observations in cotton fields in Texas, USA, showed that carbon sinks were stronger in years that were more conducive to weed growth [67]. Chamizo et al. found that the complete removal of weeds from an olive orchard resulted in a significant reduction in carbon uptake [68].

Unexpectedly, correlations existed among the changes in daily NEE of the three ecosystems. This may be due to similar trends in various environmental factors and other drivers of carbon fluxes within the same watershed. The weak correlation of NEE between the cropland and non-timber forest sites may be due to the influence of crop harvesting processes. In summary, studies on carbon sinks in small watersheds are complex due to a combination of factors.

4.3. Carbon Sink Functions in the Reshuihe River Watershed

The composition of ecosystems in a region is a crucial factor affecting carbon sinks/ sources [13,69]. In the Reshuihe River watershed, forest, cropland, and non-timber forest ecosystems accounted for 61.6%, 13.5%, and 0.27% of the total area of the Reshuihe watershed, respectively. Based on the upscaling method of carbon fluxes from the three ecosystems, the annual carbon sink of the watershed was $-52.15~\rm Gg~C~a^{-1}$. Thus, the Reshuihe River watershed is a carbon sink. In the Pallas region of northern Finland, Aurela et al. conducted a similar study in a small watershed of $105~\rm km^2$ in size (catchment area of Pallasjärvi) [13]. They calculated the carbon fluxes from four major ecosystems in the area (61% coniferous forests, 17% lakes, 13% fells, and 5% lakes) by multiplying the annual fluxes of each ecosystem by the area of the corresponding land cover class and obtained an annual carbon flux of $+5.3~\rm g~m^{-2}~a^{-1}$ for the region. This suggests that this small watershed in Finland, which was dominated by forest ecosystems, acts as a source of carbon. This highlights the importance of using multi-site eddy covariance observations to accurately determine the carbon sink function of small watersheds.

4.4. Uncertainty in Carbon Sink Estimates

The fragmented land use in Southwestern China increases the difficulty of studying carbon sinks in small watersheds. In addition to forest, cropland, and non-timber forest, the remaining land use types in the Reshuihe River watershed consist mainly of grassland ecosystems (16.6%) and aquatic ecosystems (2.2%), and the carbon fluxes of these two ecosystems are the main sources of uncertainty in carbon-balance estimations. Previous studies have shown that subtropical alpine meadow ecosystems in Southwestern China are carbon sinks [70]. On the other hand, the carbon balance of terrestrial ecosystems could be affected by the export and emission of different types of carbon through aquatic systems [71]. A study by Zhang et al. in subtropical rivers in Southwestern China showed that rivers are a source of carbon for the atmosphere (0.032 \pm 0.047 Tg C a⁻¹) [72]. Nevertheless, an analysis by Webb et al. emphasized that aquatic carbon offsets an average of 9% of NEP in forest ecosystems, and that aquatic carbon was important in ecosystems with small NEP [73]. In a study on the impact of aquatic carbon on carbon sinks in watersheds, Song et al. calculated the terrestrial and aquatic carbon fluxes in a 117 km² watershed dominated by grassland ecosystems [69]. They found that, despite the presence of aquatic carbon emissions, the carbon sink function of the region remained unchanged, and the watershed continued to maintain a net carbon uptake ($-27.7 \text{ gC m}^{-2} \text{ a}^{-1}$). Based on previous findings as such, we concluded that carbon uptake by grassland ecosystems and carbon release by aquatic ecosystems may not have a large impact on the carbon sink function in our study area.

In addition, for small watersheds that serve as both natural and social units, direct and indirect management activities may have impacts on ecosystem carbon exchange [74]. In the Reshuihe River watershed, we observed that forest ecosystems possess a strong capacity to absorb carbon, but this sink's sustainability is affected by various factors. For example,

fires cause direct carbon loss and reduce post-fire carbon sequestration capacity [75], while deforestation directly weakens ecosystem carbon sinks [74]. Fortunately, the government has invested significant resources in reducing the incidence of fires and deforestation [76,77], which has helped to enhance the ecosystem's ability to fix carbon. Additionally, widely implemented reforestation policies have compensated for carbon loss through logging and fires by promoting new growth [78]. Another concern is the age of the trees. The forests in our study area are currently experiencing rapid growth and development, resulting in a high capacity for carbon sequestration. Traditional views suggested that as forests aged, their carbon sink would cease to accumulate carbon [79]. Nevertheless, numerous studies have demonstrated that old-growth forests remain important carbon sinks [80,81]. In Southwestern China, Shu et al. discovered that subalpine primeval Abies fabri forests over 150 years old were significant carbon sinks [82], and Fei et al. found through long-term monitoring that evergreen old-growth forests were still strongly absorbing carbon [17]. Therefore, the Reshuihe River watershed forests are expected to maintain strong net carbon sequestration for an extended period of time in the future. Similarly, biomass removal from croplands and non-timber forests may eventually release some of the CO₂ back into atmosphere as it is consumed or decomposed, which may offset some of the observed net carbon sink [25,61]. This process occurs not only within watersheds, but also outside watersheds due to the marketing and distribution of harvested fruits. Therefore, a harmonized framework should be developed in the future to study the trans-regional transfer of carbon in detail. In summary, although many management-related events may affect ecosystem carbon balance, we remain positive that the Reshuihe River watershed acts as a strong carbon sink because forest ecosystems, which are less affected by management actions, are the main source of carbon sinks in the small watershed (Figure 9).

5. Conclusions

In this study, we conducted two years of observations of eddy covariance measurements to understand the carbon fluxes from forest, cropland, and non-timber forest ecosystems in the Reshuihe River watershed in Southwestern China. The results showed that all three ecosystems were annual net carbon sinks during the study period. The forest site dominated by *Pinus yunnanensis* exhibited the strongest carbon sink capacity, followed by the non-timber forest site planted with *Zanthoxylum bungeanum Maxim*, and the smallest carbon sinks were found in the cropland site planted with potatoes and maize, with average annual NEE values of -540.45 ± 52.35 , -371.0, and -82.05 ± 10.45 gC m⁻² a⁻¹, respectively.

Path analysis results showed that PAR was the most important influencing factor controlling changes in daily NEE in all three ecosystems. SVWC and T_{air} affected NEE by regulating GPP and Re. Higher SVWC promoted GPP and Re, favoring net carbon uptake. A significant decrease in GPP and Re was observed in the cropland when T_{air} was greater than 21 °C, although this did not have a significant effect on NEE.

By multiplying the annual carbon fluxes of the forest, cropland, and non-timber forest sites by the areas covered by the corresponding ecosystems, the annual carbon sink of the Reshuihe River watershed was found to be $-52.15~\rm Gg~C~a^{-1}$. This indicates that the watershed acted as a net carbon sink. Although there are some uncertainties in this estimate, based on existing research, we believe that these uncertainties are unlikely to have a significant impact on the carbon sinks of the watershed. Given the current debates in estimating carbon sinks in Southwestern China using the top-down (atmospheric inversions) approach, our study of upscaled carbon sink estimation in small watersheds using multi-site eddy covariance observations provides new insights in accurately estimating carbon balance in such environment.

Author Contributions: Methodology, W.C., H.Y., X.Z. and Z.L.; Software, W.C. and X.Z.; Validation, Y.L. (Yafeng Lu) and H.Y.; Formal analysis, W.C.; Investigation, W.C., Y.L. (Yafeng Lu), X.Z., Z.L. and Y.L. (Yanguo Liu); Data curation, W.C., Z.L. and Y.L. (Yanguo Liu); Writing—original draft, W.C.; Writing—review & editing, W.C., Y.L. (Yafeng Lu) and H.Y.; Visualization, X.Z.; Supervision, Y.L.

(Yafeng Lu); Project administration, Y.L. (Yafeng Lu); Funding acquisition, Y.L. (Yafeng Lu). All authors have read and agreed to the published version of the manuscript.

Funding: This study was supported by the National Natural Science Foundation of China for Distinguished Young Scholars (41925030) and National Natural Science Foundation of China for General Program (42171118).

Data Availability Statement: The original contributions presented in the study are included in the article, further inquiries can be directed to the corresponding author.

Conflicts of Interest: The authors declare no conflict of interest.

References

- 1. Wang, J.; Feng, L.; Palmer, P.I.; Liu, Y.; Fang, S.; Bösch, H.; ODell, C.W.; Tang, X.; Yang, D.; Liu, L. Large Chinese land carbon sink estimated from atmospheric carbon dioxide data. *Nature* **2020**, *586*, 720–723. [CrossRef]
- 2. Yang, Y.; Shi, Y.; Sun, W.; Chang, J.; Zhu, J.; Chen, L.; Wang, X.; Guo, Y.; Zhang, H.; Yu, L. Terrestrial carbon sinks in China and around the world and their contribution to carbon neutrality. *Sci. China Life Sci.* 2022, *65*, 861–895. [CrossRef] [PubMed]
- 3. IPCC AR. Climate Change 2013: The Physical Science Basis. Contribution of Working Group I to the Fifth Assessment Report of the Intergovernmental Panel on Climate Change; Cambridge University Press: New York, NY, USA, 2013; p. 1535.
- 4. Casas-Ruiz, J.P.; Bodmer, P.; Bona, K.A.; Butman, D.; Couturier, M.; Emilson, E.J.; Finlay, K.; Genet, H.; Hayes, D.; Karlsson, J. Integrating terrestrial and aquatic ecosystems to constrain estimates of land-atmosphere carbon exchange. *Nat. Commun.* 2023, 14, 1571. [CrossRef]
- 5. Ciais, P.; Bastos, A.; Chevallier, F.; Lauerwald, R.; Poulter, B.; Canadell, P.; Hugelius, G.; Jackson, R.B.; Jain, A.; Jones, M. Definitions and methods to estimate regional land carbon fluxes for the second phase of the REgional Carbon Cycle Assessment and Processes Project (RECCAP-2). *Geosci. Model Dev. Discuss.* **2020**, *15*, 1289–1316. [CrossRef]
- 6. Piao, S.; He, Y.; Wang, X.; Chen, F. Estimation of China's terrestrial ecosystem carbon sink: Methods, progress and prospects. *Sci. China Earth Sci.* **2022**, *65*, 641–651. [CrossRef]
- 7. Baldocchi, D. Measuring fluxes of trace gases and energy between ecosystems and the atmosphere—The state and future of the eddy covariance method. *Glob. Chang. Biol.* **2014**, *20*, 3600–3609. [CrossRef]
- 8. Yu, G.; Chen, Z.; Piao, S.; Peng, C.; Ciais, P.; Wang, Q.; Li, X.; Zhu, X. High carbon dioxide uptake by subtropical forest ecosystems in the East Asian monsoon region. *Proc. Natl. Acad. Sci. USA* **2014**, *111*, 4910–4915. [CrossRef]
- 9. Yao, Y.; Li, Z.; Wang, T.; Chen, A.; Wang, X.; Du, M.; Jia, G.; Li, Y.; Li, H.; Luo, W. A new estimation of China's net ecosystem productivity based on eddy covariance measurements and a model tree ensemble approach. *Agric. For. Meteorol.* **2018**, 253, 84–93. [CrossRef]
- 10. Jiang, F.; Chen, J.M.; Zhou, L.; Ju, W.; Zhang, H.; Machida, T.; Ciais, P.; Peters, W.; Wang, H.; Chen, B. A comprehensive estimate of recent carbon sinks in China using both top-down and bottom-up approaches. *Sci. Rep.* **2016**, *6*, 22130. [CrossRef]
- 11. Piao, S.; Fang, J.; Ciais, P.; Peylin, P.; Huang, Y.; Sitch, S.; Wang, T. The carbon balance of terrestrial ecosystems in China. *Nature* **2009**, 458, 1009–1013. [CrossRef]
- 12. Chen, B.; Coops, N.C. Understanding of coupled terrestrial carbon, nitrogen and water dynamics—An overview. *Sensors* **2009**, *9*, 8624–8657. [CrossRef] [PubMed]
- 13. Aurela, M.; Lohila, A.; Tuovinen, J.; Hatakka, J.; Penttilä, T.; Laurila, T. Carbon dioxide and energy flux measurements in four northern-boreal ecosystems at Pallas. *Boreal Environ. Res.* **2015**, *20*, 455–473.
- 14. Baldocchi, D.; Chu, H.; Reichstein, M. Inter-annual variability of net and gross ecosystem carbon fluxes: A review. *Agric. For. Meteorol.* **2018**, 249, 520–533. [CrossRef]
- 15. Fei, X.; Jin, Y.; Zhang, Y.; Sha, L.; Liu, Y.; Song, Q.; Zhou, W.; Liang, N.; Yu, G.; Zhang, L. Eddy covariance and biometric measurement s show that a savanna ecosystem in Southwest China is a carbon sink. *Sci. Rep.* **2017**, *7*, 41025. [CrossRef]
- Mendes, K.R.; Campos, S.; Da Silva, L.L.; Mutti, P.R.; Ferreira, R.R.; Medeiros, S.S.; Perez-Marin, A.M.; Marques, T.V.; Ramos, T.M.; de Lima Vieira, M.M. Seasonal variation in net ecosystem CO₂ exchange of a Brazilian seasonally dry tropical forest. Sci. Rep. 2020, 10, 9454. [CrossRef]
- 17. Fei, X.; Song, Q.; Zhang, Y.; Liu, Y.; Sha, L.; Yu, G.; Zhang, L.; Duan, C.; Deng, Y.; Wu, C. Carbon exchanges and their responses to temperature and precipitation in forest ecosystems in Yunnan, Southwest China. *Sci. Total Environ.* **2018**, *616*, 824–840. [CrossRef] [PubMed]
- 18. Liu, J.; Lai, D.Y. Subtropical mangrove wetland is a stronger carbon dioxide sink in the dry than wet seasons. *Agric. For. Meteorol.* **2019**, 278, 107644. [CrossRef]
- 19. Vickers, D.; Mahrt, L. Quality Control and Flux Sampling Problems for Tower and Aircraft Data. *J. Atmos. Ocean. Technol.* **1997**, 14, 512–526. [CrossRef]
- 20. Kaimal, J.C.; Finnigan, J.J. *Atmospheric Boundary Layer Flows: Their Structure and Measurement*; Oxford University Press: New York, NY, USA, 1994.
- 21. Wilczak, J.M.; Oncley, S.P.; Stage, S.A. Sonic anemometer tilt correction algorithms. *Bound. Layer Meteorol.* **2001**, 99, 127–150. [CrossRef]

22. Webb, E.K.; Pearman, G.I.; Leuning, R. Correction of flux measurements for density effects due to heat and water vapour transfer. *Q. J. R. Meteorol. Soc.* **1980**, *106*, 85–100. [CrossRef]

- 23. Burba, G. Eddy Covariance Method for Scientific, Industrial, Agricultural and Regulatory Applications: A Field Book on Measuring Ecosystem Gas Exchange and Areal Emission Rates; LI-Cor Biosciences: Lincoln, NE, USA, 2013.
- 24. Papale, D.; Reichstein, M.; Aubinet, M.; Canfora, E.; Bernhofer, C.; Kutsch, W.; Longdoz, B.; Rambal, S.; Valentini, R.; Vesala, T.; et al. Towards a standardized processing of Net Ecosystem Exchange measured with eddy covariance technique: Algorithms and uncertainty estimation. *Biogeosciences* **2006**, *3*, 571–583. [CrossRef]
- 25. Kim, K.; Daly, E.J.; Flesch, T.K.; Coates, T.W.; Hernandez-Ramirez, G. Carbon and water dynamics of a perennial versus an annual grain crop in temperate agroecosystems. *Agric. For. Meteorol.* **2022**, *314*, 108805. [CrossRef]
- 26. Reichstein, M.; Falge, E.; Baldocchi, D.; Papale, D.; Aubinet, M.; Berbigier, P.; Bernhofer, C.; Buchmann, N.; Gilmanov, T.; Granier, A.; et al. On the separation of net ecosystem exchange into assimilation and ecosystem respiration: Review and improved algorithm. *Glob. Chang. Biol.* 2005, 11, 1424–1439. [CrossRef]
- 27. Wutzler, T.; Lucas-Moffat, A.; Migliavacca, M.; Knauer, J.; Sickel, K.; Šigut, L.; Menzer, O.; Reichstein, M. Basic and extensible post-processing of eddy covariance flux data with REddyProc. *Biogeosciences* **2018**, *15*, 5015–5030. [CrossRef]
- 28. Lloyd, J.; Taylor, J.A. On the temperature dependence of soil respiration. Funct. Ecol. 1994, 8, 315–323. [CrossRef]
- 29. Leverenz, J.W.; Jarvis, P.G. Photosynthesis in Sitka spruce. VIII. The effects of light flux density and direction on the rate of net photosynthesis and the stomatal conductance of needles. *J. Appl. Ecol.* **1979**, *16*, 919–932. [CrossRef]
- 30. Knox, S.H.; Windham Myers, L.; Anderson, F.; Sturtevant, C.; Bergamaschi, B. Direct and indirect effects of tides on ecosystem-scale CO₂ exchange in a brackish tidal marsh in Northern California. *J. Geophys. Res. Biogeosci.* **2018**, 123, 787–806. [CrossRef]
- 31. You, Y.; Wang, S.; Pan, N.; Ma, Y.; Liu, W. Growth stage-dependent responses of carbon fixation process of alpine grasslands to climate change over the Tibetan Plateau, China. *Agric. For. Meteorol.* **2020**, *291*, 108085. [CrossRef]
- 32. Zhang, T.; Zhang, Y.; Xu, M.; Zhu, J.; Chen, N.; Jiang, Y.; Huang, K.; Zu, J.; Liu, Y.; Yu, G. Water availability is more important than temperature in driving the carbon fluxes of an alpine meadow on the Tibetan Plateau. *Agric. For. Meteorol.* **2018**, 256–257, 22–31. [CrossRef]
- 33. Rosseel, Y. lavaan: An R package for structural equation modeling. J. Stat. Softw. 2012, 48, 1–36. [CrossRef]
- 34. Montagnani, L.; Zanotelli, D.; Tagliavini, M.; Tomelleri, E. Timescale effects on the environmental control of carbon and water fluxes of an apple orchard. *Ecol. Evol.* **2018**, *8*, 416–434. [CrossRef] [PubMed]
- 35. Li, C.; Li, Z.; Zhang, F.; Lu, Y.; Duan, C.; Xu, Y. Seasonal dynamics of carbon dioxide and water fluxes in a rice-wheat rotation system in the Yangtze-Huaihe region of China. *Agric. Water Manag.* **2023**, 275, 107992. [CrossRef]
- 36. Xie, J.; Jia, X.; He, G.; Zhou, C.; Yu, H.; Wu, Y.; Bourque, C.P.; Liu, H.; Zha, T. Environmental control over seasonal variation in carbon fluxes of an urban temperate forest ecosystem. *Landsc. Urban Plan* **2015**, *142*, 63–70. [CrossRef]
- 37. Xing, W.; Yang, L.; Wang, W.; Yu, Z.; Shao, Q.; Xu, S.; Fu, J. Environmental controls on carbon and water fluxes of a wheat-maize rotation cropland over the Huaibei Plain of China. *Agric. Water Manag.* **2023**, 283, 108310. [CrossRef]
- 38. Wang, X.; Wang, X.; Wei, Q.; Wang, W.; Wang, S.; Huo, Z.; Lei, H. Coupling of net ecosystem CO₂ exchange and evapotranspiration of irrigated maize field in arid areas. *J. Hydrol.* **2021**, *603*, 127140. [CrossRef]
- 39. Liu, Z.; Li, K.; Xiong, K.; Li, Y.; Wang, J.; Sun, J.; Cai, L. Effects of Zanthoxylum bungeanum planting on soil hydraulic properties and soil moisture in a karst area. *Agric. Water Manag.* **2021**, 257, 107125. [CrossRef]
- 40. Wang, C.; Fu, B.; Zhang, L.; Xu, Z. Soil moisture–plant interactions: An ecohydrological review. *J. Soils Sediments* **2019**, 19, 1–9. [CrossRef]
- 41. Yuste, J.C.; Janssens, I.A.; Carrara, A.; Meiresonne, L.; Ceulemans, R. Interactive effects of temperature and precipitation on soil respiration in a temperate maritime pine forest. *Tree Physiol.* **2003**, 23, 1263–1270. [CrossRef] [PubMed]
- 42. Reichstein, M.; Tenhunen, J.D.; Roupsard, O.; Ourcival, J.M.; Rambal, S.; Dore, S.; Valentini, R. Ecosystem respiration in two Mediterranean evergreen Holm Oak forests: Drought effects and decomposition dynamics. *Funct. Ecol.* 2002, 16, 27–39. [CrossRef]
- 43. Niu, S.; Wu, M.; Han, Y.; Xia, J.; Li, L.; Wan, S. Water-mediated responses of ecosystem carbon fluxes to climatic change in a temperate steppe. *New Phytol.* **2008**, 177, 209–219. [CrossRef]
- 44. Fu, Y.; Yu, G.; Sun, X.; Li, Y.; Wen, X.; Zhang, L.; Li, Z.; Zhao, L.; Hao, Y. Depression of net ecosystem CO₂ exchange in semi-arid Leymus chinensis steppe and alpine shrub. *Agric. For. Meteorol.* **2006**, *137*, 234–244. [CrossRef]
- 45. Pingintha, N.; Leclerc, M.Y.; Beasley, J.P.; Durden, D.; Zhang, G.; Senthong, C.; Rowland, D. Hysteresis response of daytime net ecosystem exchange during drought. *Biogeosciences* **2010**, *7*, 1159–1170. [CrossRef]
- 46. Janssens, I.A.; Lankreijer, H.; Matteucci, G.; Kowalski, A.S.; Buchmann, N.; Epron, D.; Pilegaard, K.; Kutsch, W.; Longdoz, B.; Grünwald, T. Productivity overshadows temperature in determining soil and ecosystem respiration across European forests. *Glob. Chang. Biol.* 2001, 7, 269–278. [CrossRef]
- 47. Ensminger, I.; Busch, F.; Huner, N.P.A. Photostasis and cold acclimation: Sensing low temperature through photosynthesis. *Physiol. Plant.* **2006**, 126, 28–44. [CrossRef]
- 48. Hudson, J.; Henry, G.; Cornwell, W.K. Taller and larger: Shifts in Arctic tundra leaf traits after 16 years of experimental warming. *Glob. Chang. Biol.* **2011**, *17*, 1013–1021. [CrossRef]
- 49. Wang, L.; Chen, W. A CMIP5 multimodel projection of future temperature, precipitation, and climatological drought in China. *Int. J. Climatol.* **2014**, 34, 2059–2078. [CrossRef]

50. Yan, J.; Zhang, Y.; Yu, G.; Zhou, G.; Zhang, L.; Li, K.; Tan, Z.; Sha, L. Seasonal and inter-annual variations in net ecosystem exchange of two old-growth forests in southern China. *Agric. For. Meteorol.* **2013**, *182*, 257–265. [CrossRef]

- 51. Guan, D.; Wu, J.; Zhao, X.; Han, S.; Yu, G.; Sun, X.; Jin, C. CO₂ fluxes over an old, temperate mixed forest in northeastern China. *Agric. For. Meteorol.* **2006**, *137*, 138–149. [CrossRef]
- 52. Ilvesniemi, H.; Levula, J.; Ojansuu, R.; Kolari, P.; Kulmala, L.; Pumpanen, J.; Launiainen, S.; Vesala, T.; Nikinmaa, E. Long-term measurements of the carbon balance of a boreal Scots pine dominated forest ecosystem. *Boreal Environ. Res.* **2009**, 14, 731–753.
- 53. Maseyk, K.S.; Lin, T.; Rotenberg, E.; Grunzweig, J.M.; Schwartz, A.; Yakir, D. Physiology-phenology interactions in a productive semi-arid pine forest. *New Phytol.* **2008**, *178*, 603–616. [CrossRef]
- 54. Dore, S.; Montes Helu, M.; Hart, S.C.; Hungate, B.A.; Koch, G.W.; Moon, J.B.; Finkral, A.J.; Kolb, T.E. Recovery of ponderosa pine ecosystem carbon and water fluxes from thinning and stand-replacing fire. *Glob. Chang. Biol.* **2012**, *18*, 3171–3185. [CrossRef]
- 55. Wharton, S.; Falk, M. Climate indices strongly influence old-growth forest carbon exchange. *Environ. Res. Lett.* **2016**, *11*, 44016. [CrossRef]
- Noormets, A.; Gavazzi, M.J.; McNulty, S.G.; Domecj, C.; Sun, G.E.; King, J.S.; Chen, J. Response of carbon fluxes to drought in a coastal plain loblolly pine forest. Glob. Chang. Biol. 2010, 16, 272–287. [CrossRef]
- 57. Bracho, R.; Starr, G.; Gholz, H.L.; Martin, T.A.; Cropper, W.P.; Loescher, H.W. Controls on carbon dynamics by ecosystem structure and climate for southeastern US slash pine plantations. *Ecol. Monogr.* **2012**, *82*, 101–128. [CrossRef]
- 58. Dolman, A.J.; Moors, E.J.; Elbers, J.A. The carbon uptake of a mid latitude pine forest growing on sandy soil. *Agric. For. Meteorol.* **2002**, *111*, 157–170. [CrossRef]
- 59. Zeri, M.; Sa, L.D.; Manzi, A.O.; Araujo, A.C.; Aguiar, R.G.; von Randow, C.; Sampaio, G.; Cardoso, F.L.; Nobre, C.A. Variability of carbon and water fluxes following climate extremes over a tropical forest in southwestern Amazonia. *PLoS ONE* **2014**, *9*, e88130. [CrossRef] [PubMed]
- 60. Barr, A.G.; Black, T.A.; Hogg, E.H.; Griffis, T.J.; Morgenstern, K.; Kljun, N.; Theede, A.; Nesic, Z. Climatic controls on the carbon and water balances of a boreal aspen forest, 1994–2003. *Glob. Chang. Biol.* **2007**, *13*, 561–576. [CrossRef]
- 61. Peng, X.; Wang, Y.; Ma, J.; Liu, X.; Gu, X.; Cai, H. Seasonal variation and controlling factors of carbon balance over dry semi-humid cropland in Guanzhong Plain. *Eur. J. Agron.* **2023**, *149*, 126912. [CrossRef]
- 62. Wang, H.; Li, X.; Xiao, J.; Ma, M.; Tan, J.; Wang, X.; Geng, L. Carbon fluxes across alpine, oasis, and desert ecosystems in northwestern China: The importance of water availability. *Sci. Total Environ.* **2019**, 697, 133978. [CrossRef]
- 63. Li, J.; Yu, Q.; Sun, X.; Tong, X.; Ren, C.; Wang, J.; Liu, E.; Zhu, Z.; Yu, G. Carbon dioxide exchange and the mechanism of environmental control in a farmland ecosystem in North China Plain. *Sci. China Ser. D Earth Sci.* **2006**, 49, 226–240. [CrossRef]
- 64. Law, B.E.; Falge, E.; Gu, L.; Baldocchi, D.D.; Bakwin, P.; Berbigier, P.; Davis, K.; Dolman, A.J.; Falk, M.; Fuentes, J.D. Environmental controls over carbon dioxide and water vapor exchange of terrestrial vegetation. *Agric. For. Meteorol.* **2002**, *113*, 97–120. [CrossRef]
- 65. Suyker, A.E.; Verma, S.B. Coupling of carbon dioxide and water vapor exchanges of irrigated and rainfed maize—soybean cropping systems and water productivity. *Agric. For. Meteorol.* **2010**, *150*, 553–563. [CrossRef]
- 66. Anthoni, P.M.; Freibauer, A.; Kolle, O.; Schulze, E. Winter wheat carbon exchange in Thuringia, Germany. *Agric. For. Meteorol.* **2004**, *121*, 55–67. [CrossRef]
- 67. Menefee, D.; Rajan, N.; Cui, S.; Bagavathiannan, M.; Schnell, R.; West, J. Carbon exchange of a dryland cotton field and its relationship with PlanetScope remote sensing data. *Agric. For. Meteorol.* **2020**, 294, 108130. [CrossRef]
- 68. Chamizo, S.; Serrano-Ortiz, P.; López-Ballesteros, A.; Sánchez-Cañete, E.P.; Vicente-Vicente, J.L.; Kowalski, A.S. Net ecosystem CO₂ exchange in an irrigated olive orchard of SE Spain: Influence of weed cover. *Agric. Ecosyst. Environ.* **2017**, 239, 51–64. [CrossRef]
- 69. Song, C.; Wang, G.; Hu, Z.; Zhang, T.; Huang, K.; Chen, X.; Li, Y. Net ecosystem carbon budget of a grassland ecosystem in central Qinghai-Tibet Plateau: Integrating terrestrial and aquatic carbon fluxes at catchment scale. *Agric. For. Meteorol.* **2020**, 290, 108021. [CrossRef]
- 70. Wang, L.; Liu, H.; Sun, J.; Feng, J. Water and carbon dioxide fluxes over an alpine meadow in southwest China and the impact of a spring drought event. *Int. J. Biometeorol.* **2016**, *60*, 195–205. [CrossRef] [PubMed]
- 71. Butman, D.; Stackpoole, S.; Stets, E.; McDonald, C.P.; Clow, D.W.; Striegl, R.G. Aquatic carbon cycling in the conterminous United States and implications for terrestrial carbon accounting. *Proc. Natl. Acad. Sci. USA* **2016**, *113*, 58–63. [CrossRef]
- 72. Zhang, T.; Li, J.; Pu, J.; Yuan, D. Carbon dioxide exchanges and their controlling factors in Guijiang River, SW China. *J. Hydrol.* **2019**, *578*, 124073. [CrossRef]
- 73. Webb, J.R.; Santos, I.R.; Maher, D.T.; Finlay, K. The importance of aquatic carbon fluxes in net ecosystem carbon budgets: A catchment-scale review. *Ecosystems* **2019**, 22, 508–527. [CrossRef]
- 74. Ruehr, S.; Keenan, T.F.; Williams, C.; Zhou, Y.; Lu, X.; Bastos, A.; Canadell, J.G.; Prentice, I.C.; Sitch, S.; Terrer, C. Evidence and attribution of the enhanced land carbon sink. *Nat. Rev. Earth Environ.* **2023**, *4*, 518–534. [CrossRef]
- 75. Sun, Q.; Meyer, W.S.; Koerber, G.R.; Marschner, P. Rapid recovery of net ecosystem production in a semi-arid woodland after a wildfire. *Agric. For. Meteorol.* **2020**, 291, 108099. [CrossRef]
- 76. Xiong, Q.; Luo, X.; Liang, P.; Xiao, Y.; Xiao, Q.; Sun, H.; Pan, K.; Wang, L.; Li, L.; Pang, X. Fire from policy, human interventions, or biophysical factors? Temporal–spatial patterns of forest fire in southwestern China. For. Ecol. Manag. 2020, 474, 118381. [CrossRef]
- 77. Ren, G.; Young, S.S.; Wang, L.; Wang, W.; Long, Y.; Wu, R.; Li, J.; Zhu, J.; Yu, D.W. Effectiveness of China's national forest protection program and nature reserves. *Conserv. Biol.* **2015**, *29*, 1368–1377. [CrossRef] [PubMed]

78. Zhang, X.M.; Brandt, M.; Yue, Y.M.; Tong, X.W.; Wang, K.L.; Fensholt, R. The carbon sink potential of southern China after two decades of afforestation. *Earth's Future* **2022**, *10*, e2022E–e2674E. [CrossRef] [PubMed]

- 79. Kira, T.; Shidei, T. Primary production and turnover of organic matter in different forest ecosystems of the western Pacific. *Jpn. J. Ecol.* **1967**, 17, 70–87.
- 80. Tan, Z.; Zhang, Y.; Schaefer, D.; Yu, G.; Liang, N.; Song, Q. An old-growth subtropical Asian evergreen forest as a large carbon sink. *Atmos. Environ.* **2011**, *45*, 1548–1554. [CrossRef]
- 81. Luyssaert, S.; Schulze, E.; Börner, A.; Knohl, A.; Hessenmöller, D.; Law, B.E.; Ciais, P.; Grace, J. Old-growth forests as global carbon sinks. *Nature* **2008**, *455*, 213–215. [CrossRef]
- 82. Shu, S.; Zhu, W.; Wang, W.; Jia, M.; Zhang, Y.; Sheng, Z. Effects of tree size heterogeneity on carbon sink in old forests. *For. Ecol. Manag.* **2019**, 432, 637–648. [CrossRef]

Disclaimer/Publisher's Note: The statements, opinions and data contained in all publications are solely those of the individual author(s) and contributor(s) and not of MDPI and/or the editor(s). MDPI and/or the editor(s) disclaim responsibility for any injury to people or property resulting from any ideas, methods, instructions or products referred to in the content.